PCCP

RSC Publishing

PAPER

View Article Online
View Journal | View Issue

Cite this: *Phys. Chem. Chem. Phys.*, 2013, **15**, 11362

Electrochemical synthesis of vertically aligned zinc nanowires using track-etched polycarbonate membranes as templates

Z. Liu,[a] S. Zein El Abedin,[ab] M. S. Ghazvini[a] and F. Endres*[a]

Received 2nd April 2013,
Accepted 14th May 2013

DOI: 10.1039/c3cp51325d

www.rsc.org/pccp

In the present paper, vertically aligned arrays of zinc nanowires were synthesized by electrochemical deposition into ion track-etched polycarbonate membranes in the ionic liquid electrolyte 1-ethyl-3-methylimidazolium trifluoromethylsulfonate ([EMIm]TfO)/$Zn(TfO)_2$. Cyclic voltammetry and chronoamperometry were performed to investigate the electrochemical growth of zinc nanowires inside of the membranes. The transport processes and mechanisms of the nanowire growth in the membranes are also discussed. A supporting zinc or copper layer was deposited on the sputtered side in order to make the back layer thick enough to stabilize the wires. Zinc nanowires with a diameter of 90 nm and a length of up to 18 μm were obtained after removing the template. Furthermore, short nanowires with lengths less than 5 μm and a sandwich-like structure with nanowires in the middle were also synthesized. Vertically aligned zinc nanowire structures on such a substrate might be a potential anode candidate for future generation lithium ion batteries.

1. Introduction

Metal nanowires show a variety of quite interesting physical and chemical properties, which are not seen in bulk materials, such as superconductivity, enhanced mechanical properties and coercivities and remnant magnetization.[1,2] The synthesis of metal nanowire arrays has attracted more attention in recent years because of their potential applications in batteries, catalysis and nanoscale electronic devices.[3–5] Several methods have been employed to synthesize metal nanowires, including electrochemical deposition, physical/chemical vapor deposition, and vapor–liquid–solid growth.[6–8] In this context the electrochemical deposition into nanoporous templates is a promising process to prepare metal nanowire arrays as electrodeposition is relatively simple concerning the experimental requirements. Furthermore, the composition, dimensions and the length of the nanowires can be well controlled by electrochemical methods.[9–11] Commercially available anodic aluminum oxide (AAO) and ion track-etched polymer membranes are widely used as templates. The polymer templates are fabricated by irradiation of the membranes with heavy ions followed by etching with chemicals. The pores are usually randomly distributed across the surface. Prior to electrodeposition, a conductive metal layer has to be applied on one side of the membrane to serve as an electrode for the nanowire growth. Compared to AAO, porous polymer membranes are chemically stable in many electrolytes including strong acidic and alkaline solutions.[12] Furthermore, the templates can be easily removed by dissolving them in dichloromethane.

It was reported that Zn nanowires exhibit superconducting properties[13,14] and zinc nanowire composites exhibit superior magnetoresistance and thermopower properties.[15] Furthermore, zinc nanowires are expected to have some potential as host materials for lithium ion batteries or zinc/air batteries. Free-standing zinc nanowire arrays would offer better accommodation of large volume changes during lithium insertion and extraction processes.

The synthesis of Zn nanowires, nanotubes, and nanobelts was reported recently.[16–18] However, the reported nanostructures were not free-standing on the substrate, and to the best of our knowledge there is no report on the synthesis of free-standing zinc nanostructures hitherto.

Ionic liquids (ILs) are known for their low vapor pressure and for their usually large electrochemical windows and they are quite intensively investigated as electrolytes.[19,20] There are many prospects of using ionic liquids as electrolytes as they avoid hydrogen evolution and allow the deposition of a range of

[a] *Institute of Electrochemistry, Clausthal University of Technology, Arnold-Sommerfeld-Strasse 6, 38678 Clausthal-Zellerfeld, Germany. E-mail: frank.endres@tu-clausthal.de; Fax: +49 5323 722460; Tel: +49 5323 722980*

[b] *Electrochemistry and Corrosion Laboratory, National Research Centre, Dokki, Cairo, Egypt*

reactive elements such as Al, Ga, Si, Ge, Ta, and maybe other ones, which are difficult or impossible to deposit in water.[21] The deposition of zinc from $AlCl_3$-based ionic liquids was extensively studied by Sun *et al.*[22,23] and by Abbott *et al.*[24,25] The effect of additives on zinc electrodeposition was also studied.[26–28] Recently, we could show that the electrodeposition of zinc films from 1-butyl-1-methylpyrrolidinium trifluoromethylsulfonate, $[Py_{1,4}]TfO$, and from 1-ethyl-3-methylimidazolium trifluoromethylsulfonate, [EMIm]TfO, is quite easy at room temperature[29] and even macroporous zinc structures as a potential material for batteries could be obtained.[30] Zinc nanowires are also an attractive anode host material for lithium/air or lithium ion batteries, zinc nanowires themselves possibly for zinc/air batteries.

In the present paper, vertically aligned arrays of zinc nanowires are made using ion track-etched polycarbonate membranes as templates. A copper or gold supporting layer serves as the working electrode, and the zinc nanowires are grown inside of the cylindrical nanochannels of the templates. The results show that the nanowire diameter is about 90 nm and the length can be up to 18 μm, depending on the experimental conditions. An about 7 μm thick supporting layer of zinc or copper is electrodeposited on the sputtered side of the PC membrane. The cyclic voltammograms show the typical zinc reduction and oxidation peaks. The mechanism of the nanowire growth in the ion-track etched polymer membrane is also investigated by chronoamperometry.

2. Experimental

Zinc trifluoromethylsulfonate ($Zn(TfO)_2$) powder (IO-LI-TEC, Germany, 99%) and copper(I) chloride powder (Sigma-Aldrich, American, 99.99%) were used as zinc and copper sources for electrochemical deposition, respectively. The ionic liquids 1-ethyl-3-methylimidazolium trifluoromethylsulfonate, [EMIm]TfO, and 1-ethyl-3-methylimidazolium dicyanamide, [EMIm]DCA, were obtained from IO-LI-TEC, Germany. The amount of impurities (Li^+, Cl^-) in the liquids was less than 100 ppm. Liquids with the triflate ion can contain several hundred ppm of trifluoromethylsulfonic acid. The ionic liquids were dried under vacuum at 120 °C to water contents of below 3 ppm and stored in closed bottles in an argon filled glove box (OMNI-LAB from Vacuum Atmospheres) before using. The concentration is 0.2 M for $Zn(TfO)_2$ in [EMIm]TfO and 1 M for CuCl in [EMIm]DCA, respectively.

Cyclic voltammetry and electrodeposition experiments were performed in the glove box using a classical three-electrode cell setup. The electrochemical cell made of polytetrafluoroethylene (Teflon) was clamped over a Teflon covered Viton o-ring, thus yielding a geometric surface area of 0.3 cm^2.

Track-etched polycarbonate (PC) membranes with a nominal thickness of 21 μm, an average pore diameter of 90 nm and pore densities of 10^9 cm^{-2} (Ion Track Technology for Innovative Products, IT4IP, Belgium) were used as templates. A thin layer of Au or of Cu (~100 nm thick) was sputtered on the reverse side of the templates serving as the working electrode. A platinum wire (Alfa, 99.99%) and a zinc wire (Alfa, 99.99%) were used as a counter and quasi reference electrode, respectively, for zinc deposition. The reference and counter electrodes were directly immersed in the solutions without using a separate compartment. A thick supporting zinc or copper layer is deposited on the sputtered side of the membranes. Copper wires were used both as counter and reference electrodes for copper deposition. A 10 mL glass beaker was employed as an electrochemical cell for the supporting layer deposition. The electrochemical measurements were carried out using a PARSTAT 2263 potentiostat/galvanostat controlled by PowerCV and PowerStep software.

After deposition, the membranes were rinsed with isopropanol to remove the ionic liquid and subsequently the membranes were removed by dissolving them in dichloromethane (CH_2Cl_2, AR, Merck). A high resolution SEM (Carl Zeiss DSM 982 Gemini) was used to characterize the surface morphology. Contact angle measurements were performed using a Krüss DSA100S system for sessile droplet analysis (Krüss GmbH, Hamburg, Germany).

3. Results and discussion

Fig. 1a shows a top view SEM micrograph of the track-etched PC membranes. The membranes have rather a low porosity which is usually less than 15% and the pores are randomly distributed in the membranes. In our experiment, the membranes have a nominal pore diameter of 90 nm and a pore density of 10^9 cm^{-2}. Furthermore, Fig. 1 shows that double or triple pores are present, too. A contact angle measurement, as shown in the inset of Fig. 1a, reveals that the ionic liquid well wets the membrane, which is quite important for the homogeneous growth of the nanowires inside of the membrane. Prior to deposition, a thin layer of Au or of Cu was sputtered on the reverse side of the templates to act as a supporting electrode. The thickness of the sputtered Au or Cu was roughly 100 nm and importantly the pores are not sealed by this

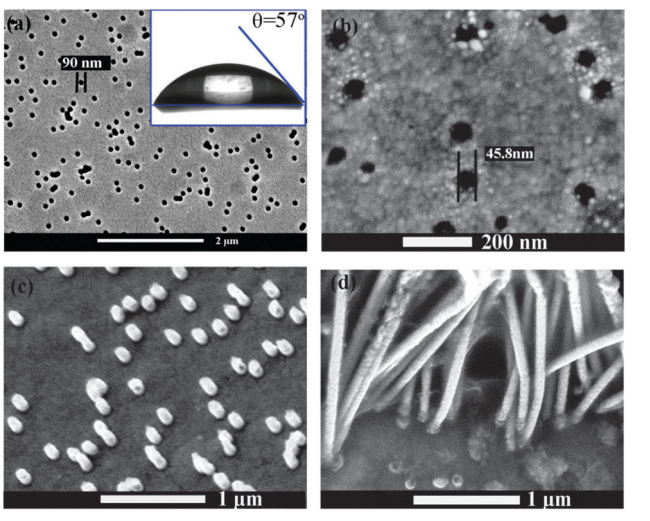

Fig. 1 SEM micrographs of (a) the polycarbonate membrane and contact angle of 0.2 M $Zn(TfO)_2$–[EMIm]TfO solutions on the membrane (inset picture), (b) the back side of the membrane after sputtering with gold, (c) back side of the sputtered gold after removing the membrane and (d) interface of the sputtered gold and zinc nanowire.

process, only the diameter is decreased to ~46 nm (Fig. 1b with sputtered Au). However, after dissolving of the membranes with dichloromethane, small Au islands or even wires can be found as shown in Fig. 1c (with sputtered Au). Similar results were also found with the sputtered copper surface. These results show that to some extent the Au or Cu particles from sputtering went inside the pore during the sputtering process and formed small islands or wires in the pore walls near the pore's surface. These small islands or even wires will serve as a special kind of nanoelectrodes for the growth of nanowires. The SEM image in Fig. 1d shows the interface between the gold substrate and the base of the nanowires. The nanowires shown in Fig 1d were obtained at a potential of −0.5 V *versus* a quasi Zn reference electrode for 2 h. The Zn nanowires will grow on these islands or wires, therefore the connection will depend on the interaction between the sputtered metal layer and the deposited metal itself. An alloy between the supporting metal and the deposited metal will improve the mechanical stability of the final electrode material. Once the template is removed, the nanowires should be free-standing. Zn alloys well with both gold and copper and it can be expected that the nanowires are free-standing as will be shown below.

The cyclic voltammograms of 0.2 M $Zn(TfO)_2$ in [EMIm]TfO on a sputtered gold surface and inside of the PC membranes are presented in Fig. 2. In the latter case the sputtered side of the membrane was pressed on a gold electrode and deposition of Zn occurred through the membrane. The electrode potential was scanned from the open circuit potential (OCP) to −1 V, then up to +1 V in the reverse scan and finally back to the former OCP with a scan rate of 10 mV s^{-1}. Cathodic waves are observed at about −0.5 V (c1) in both cases, corresponding to the reduction of Zn^{2+} to Zn. The anodic peaks at about +0.4 V (a1) are ascribed to the stripping of Zn. In both cases, a current loop was found in the deposition regime indicating a nucleation process. The CVs show that the deposited zinc is electrochemically active and the wires exist in the form of the actual reactive metal with the IL probably protecting it from self corrosion.

The cyclic voltammograms recorded under the same conditions but on the sputtered copper surface and inside of the Cu sputtered

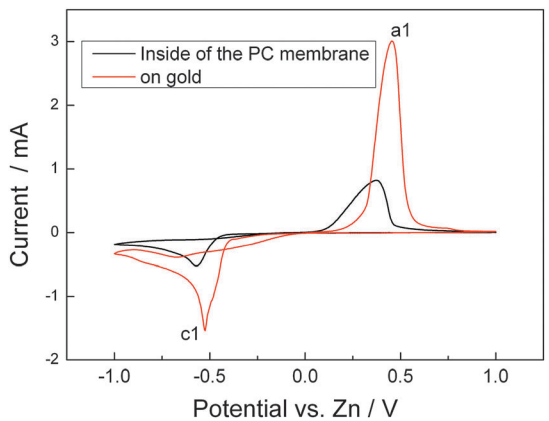

Fig. 2 CVs of 0.2 M $Zn(TfO)_2$ in [EMIm]TfO on gold and inside of the PC membrane at room temperature. Scan rate: 10 mV s^{-1}.

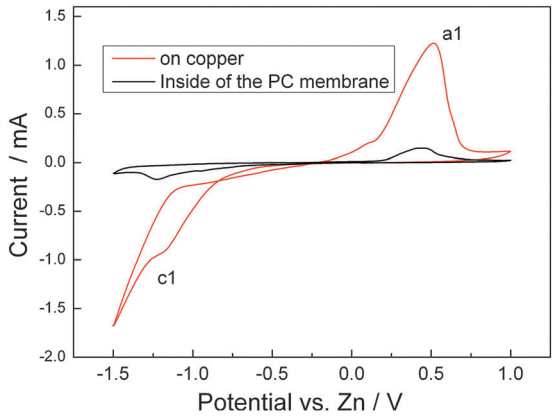

Fig. 3 CVs of 0.2 M $Zn(TfO)_2$ in [EMIm]TfO on copper and inside of the PC membrane at room temperature. Scan rate: 10 mV s^{-1}.

PC membranes are shown in Fig. 3. The CVs show the typical zinc deposition (c1) and stripping peaks (a1) as well. Compared to Fig. 2, the potential for Zn deposition is more negative in both cases on copper than on gold under the same experimental conditions. Furthermore, a current loop in the deposition regime was only found on the sputter deposited copper layers indicating a nucleation process, while such a loop was not found for deposition inside of the membranes. In both experiments the current on the sputtered side was almost 4 times higher than the one inside of the PC membranes. Such a ratio of currents is not in direct agreement with the one calculated from the porosity. Similar results were also reported for Co and Ni nanowires made in aqueous solutions.[31] In any case this result shows that the mass transport in the confined space of the nanochannels may have an effect on the growth of the nanowires.

The growth mechanism of nanowires in aqueous solutions is known and was studied by several authors.[32,33] In the present study, chronoamperometry measurements were performed to investigate the growth mechanism of Zn nanowires inside of the membranes at a constant deposition potential of $E = -0.5$ V *versus* a quasi Zn reference electrode on the Au-sputtered membrane. The current–time curve depicted in Fig. 4 can be divided into three stages. In stage 1, once the potential was applied, the nucleation occurs at the electrode–electrolyte interface forming a thin zinc layer at the bottom of the pores. The current increases first and decreases subsequently due to diffusion control. The diffusion processes are surely different from the conditions of a planar substrate due to the confined space inside of the templates. Subsequently, in stage 2, the current increases which is attributed to the proceeding growth in the pores towards the surface of the membranes. Growth proceeds until the pores are filled. Beyond this in stage 3, the deposit will now grow out of the templates by firstly forming hemispherical caps on top of the wires and then a more or less planar layer forms over the whole of the template surface. Correspondingly, the current increases first rapidly followed by a decrease due to the diffusion control. We refrain here from an overinterpretation of the chronoamperogram as also varying solvation layer effects might occur possibly influencing the

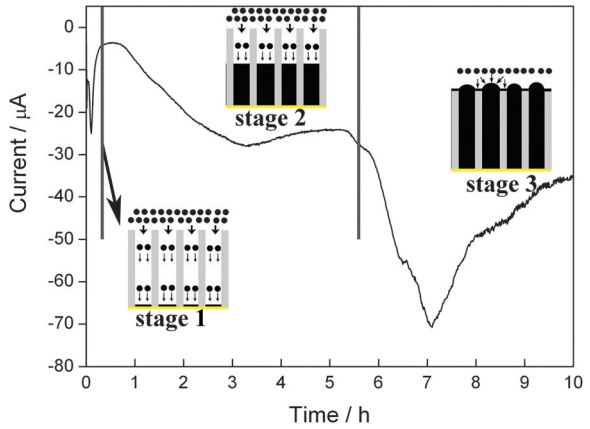

Fig. 4 Cathodic current as a function of time for the potentiostatic deposition of Zn at a potential of −0.5 V *versus* Zn inside of the Au-sputtered polycarbonate membrane from 0.2 M $Zn(TfO)_2$–[EMIm]TfO. The inset pictures display three different stages of the growth process: stage 1, Zn nucleation and formation of a thin layer on the surface; stage 2, Zn grows in the pores; stage 3, the pores are completely filled, then forming hemispherical caps on top of the wires and finally over the whole membrane.

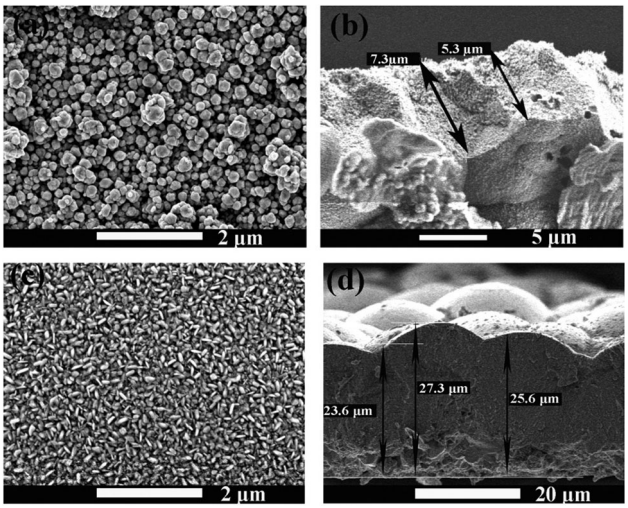

Fig. 6 Top-view SEM micrographs of Cu deposits formed in 1 M CuCl in [EMIm]DCA at a potential of −0.6 V *versus* Zn for 3 h on sputtered gold (a) and on sputtered copper (c). Cross-section of the samples is shown on gold (b) and on copper (d), respectively.

deposition process. The potentiostatic current–time curve recorded on a Cu-sputtered template was similar to that of the Au-sputtered template (the results are not shown).

Although the feasibility has been shown, the sputtered layer alone is not thick enough to allow an array of free standing nanowires. Once the template is removed in dichloromethane, the sputtered layer will break into pieces or enroll. Consequently, it is quite difficult to collect the nanowires. Therefore, a thick supporting layer is needed on the sputtered side to support the nanowires. For this purpose, firstly, a layer of Zn was deposited on the sputtered Au or Cu surface, while the other side of the membrane was isolated from the electrolyte using a PTFE (Teflon) tape. Top and cross-section views of such Zn deposits made on the Au or Cu surface are shown in Fig. 5.

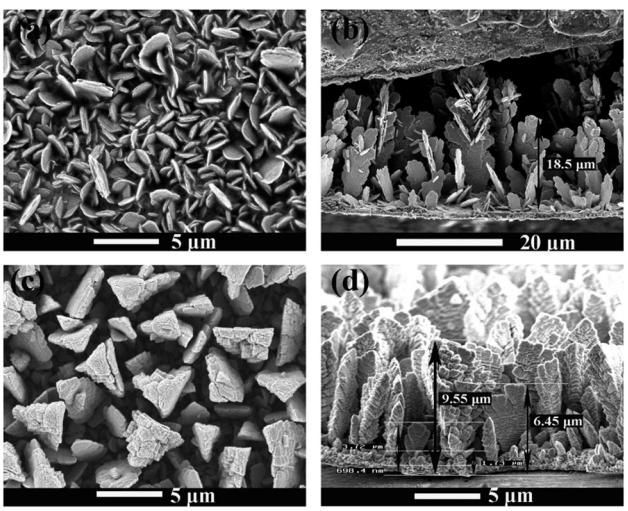

Fig. 5 Top-view SEM micrographs of Zn deposits formed in 0.2 M $Zn(TfO)_2$ in [EMIm]TfO at a potential of −0.5 V *versus* Zn for 2 h on sputtered gold (a) and on sputtered copper (c). Cross-section of the samples is shown in (b) and (d) on gold and on copper, respectively.

The Zn deposits obtained on the sputtered gold surface appear to have a platelike morphology, with the plate rather perpendicular to the surface. This growth is comparable to the one on a planar gold substrate.[29] Furthermore, the particle size of the Zn deposit on copper is larger than the one on gold. The thickness of zinc on gold and on copper was 18.5 μm and 9.5 μm, respectively. In both cases a dendritic structure formed which does not make this layer suitable as a supporting layer, it is simply too brittle. Therefore, a thick layer of copper was deposited alternatively on both sputtered Au and Cu layers from 1 M CuCl–[EMIm]DCA solutions. The advantage of depositing a layer of copper is that it can be directly used as a current collector. As shown in Fig. 6, the thickness of the Cu layer can be more than 25 μm and the surface shows a dense structure. Thus, copper is quite a good candidate material as a supporting layer for zinc nanowires. It should be mentioned here that many factors can influence the morphology of the deposits such as concentration, current density, and temperature.

Zinc nanowire arrays are of interest for applications in nanoelectronic devices; furthermore, vertically aligned zinc nanowire arrays on a conductive substrate are expected to have a good performance in batteries due to their high surface area and their good electron conductivity.[34] However, until now published zinc nanowires are randomly oriented, whereas in the present paper free-standing zinc nanowire arrays are in the focus of our interest. SEM micrographs of Zn nanowires obtained potentiostatically at a potential of −0.5 V for 6 h (on Au-sputtered) and −1.0 V for 4 h (on Cu-sputtered), respectively, are shown in Fig. 7 and 8. In both cases Cu was electrochemically deposited on the sputtered membranes as a support structure of the nanowires. Fig. 7a and 8a show a top view of the vertically aligned Zn nanowire arrays. The zinc wires are practically free-standing and perpendicular to the substrate with a high aspect ratio. But, the Zn nanowire arrays are also bunched together as clearly seen from Fig. 7b and 8b, and this

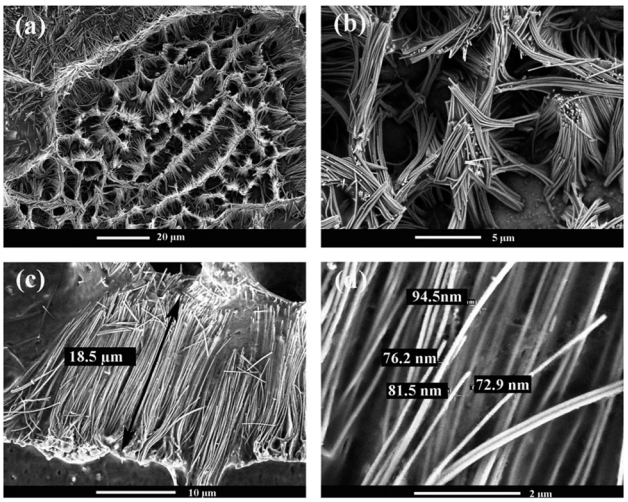

Fig. 7 (a) Top-view SEM micrograph of Zn nanowires obtained after dissolution of the polycarbonate membrane from 0.2 M $Zn(TfO)_2$–[EMIm]TfO solutions on sputtered gold with a copper supporting layer at a potential of −0.5 V *versus* Zn for 6 h. (b) Top view of the Zn nanowires with higher magnification. (c) SEM micrograph of the length of the nanowires and (d) SEM micrograph of the diameter of the nanowires.

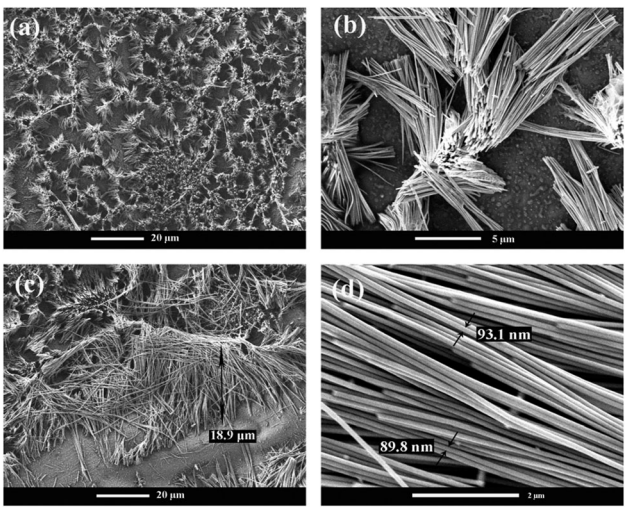

Fig. 8 (a) Top-view SEM micrograph of Zn nanowires obtained after dissolution of the polycarbonate membrane from 0.2 M $Zn(TfO)_2$–[EMIm]TfO solutions on sputtered copper with a copper supporting layer at a potential of −1.0 V *versus* Zn for 4 h. (b) Top view of the Zn nanowires with higher magnification. (c) SEM micrograph of the length of the nanowires and (d) SEM micrograph of the diameter of the nanowires.

effect increases with increasing length of the nanowires. Higher magnification SEM micrographs given in Fig. 7c and 8c show that the length of the nanowires is about 19 μm in both cases. The length of the wires, as can be seen from Fig. 7a in the corner and in Fig. 8c, is not really uniform. One possible reason is that the pores in the commercial membranes are not aligned perfectly parallel but rather have a certain angular distribution. The SEM images in Fig. 7d and 8d show that the diameters of the zinc nanowires in the middle are almost equal to the ones of the templates. Only at or near the top end of the nanowires

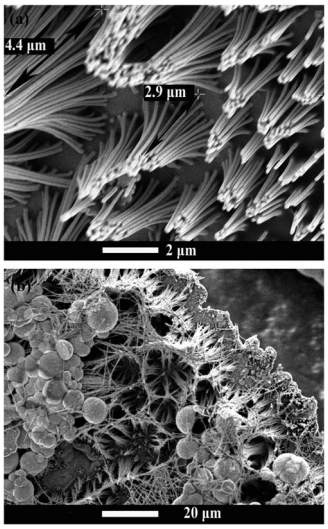

Fig. 9 SEM micrographs of free-standing Zn nanowires (a) and a sandwich-like structure (b) obtained from 0.2 M $Zn(TfO)_2$–[EMIm]TfO solutions by electrodeposition at a potential of −1.0 V *versus* Zn for 2 h and 8 h, respectively, on the copper sputtered membranes with a copper supporting layer.

the diameter is a little smaller. The diameter is about 75 nm close to the top end and 94 nm in the middle as shown in Fig. 7d, more or less in agreement with the nominal pore size.

The length of the nanowires can be well controlled by the deposition time. Fig. 9 displays SEM micrographs of free-standing zinc nanowires and of sandwich-like structures obtained at a potential of −1.0 V for 2 h and 8 h, respectively, on the copper sputtered membranes with an electrodeposited copper supporting layer. Vertically aligned zinc nanowire arrays with a length of less than 5 μm are obtained in the first case as shown in Fig. 9a. The bottoms of the wires are well separated from each other, while the tops are stuck together forming bunch-like structures. By prolonging the deposition time to 8 h (Fig. 8b) the pores are completely filled up with electrodeposited zinc and finally a thick film is grown over the surface of the template, consistent with the qualitative description of the chronoamperometry measurements. Both the short nanowires and the sandwich-like structure with nanowires in the middle might be of some interest in the field of supercapacitors or catalysis, especially as they can be fully modified in the chemical process.

4. Conclusions

In summary, we have demonstrated a comparably simple and effective approach to produce vertically aligned Zn nanowires from 1-ethyl-3-methylimidazolium trifluoromethylsulfonate/zinc triflate electrolytes by electrochemical deposition into ion track-etched polycarbonate membranes. Both the cyclic voltammograms and chronoamperometry measurements show the complicated diffusion and transport process of the Zn^{2+} inside of the nanochannels. A supporting zinc or copper layer was deposited on the sputtered side from ionic liquids in order to make the wires free standing. The SEM results show that the

diameter of the obtained zinc nanowires is about 90 nm, which is the same as the nominal diameter of the pores, and wire lengths of up to 18 μm could be obtained by controlling the deposition time. Furthermore, short nanowires with lengths of less than 5 μm and sandwich-like structures with nanowires in the middle are also synthesized.

Acknowledgements

Financial support from BMBF project AKUZIL is gratefully acknowledged.

References

1 J. I. Pascual, J. Mendez, J. Gomezherrero, A. M. Baro, N. Garcia, U. Landman, W. D. Luedtke, E. N. Bogachek and H. P. Cheng, *Science*, 1995, **267**, 1793.
2 T. M. Whitney, J. S. Jiang, P. C. Searson and C. L. Chien, *Science*, 1993, **261**, 1316.
3 S. Zein El Abedin, A. Garsuch and F. Endres, *Aust. J. Chem.*, 2012, **65**, 1529.
4 P. Christopher and S. Linic, *J. Am. Chem. Soc.*, 2008, **130**, 11264.
5 X. F. Duan, Y. Huang, Y. Cui, J. F. Wang and C. M. Lieber, *Nature*, 2001, **409**, 66.
6 T. R. Kline, M. Tian, J. Wang, A. Sen, M. W. H. Chan and T. E. Mallouk, *Inorg. Chem.*, 2006, **45**, 7555.
7 B. A. Wacaser, K. A. Dick, J. Johansson, M. T. Borgstrom, K. Deppert and L. Samuelson, *Adv. Mater.*, 2009, **21**, 153.
8 K. W. Kolasinski, *Curr. Opin. Solid State Mater. Sci.*, 2006, **10**, 182.
9 S. Zein El Abedin and F. Endres, *ChemPhysChem*, 2012, **13**, 250.
10 X. Dou, Y. Zhu, X. Huang, L. Li and G. Li, *J. Phys. Chem. B*, 2006, **110**, 21572.
11 C. Frantz, N. Stein, Y. Zhang, E. Bouzy, O. Picht, M. E. Toimil-Molares and C. Boulanger, *Electrochim. Acta*, 2012, **69**, 30.
12 M. Ulbricht, *Polymer*, 2006, **47**, 2217.
13 J. G. Wang, M. L. Tian, N. Kumar and T. E. Mallouk, *Nano Lett.*, 2005, **5**, 1247.
14 M. Tian, N. Kumar, S. Xu, J. Wang, J. S. Kurtz and M. H. W. Chan, *Phys. Rev. Lett.*, 2005, **95**, 076802.
15 J. P. Heremans, C. M. Thrush, D. T. Morelli and M. C. Wu, *Phys. Rev. Lett.*, 2003, **91**, 076804.
16 Y. J. Chen, B. Chi, H. Z. Zhang, H. Chen and Y. Chen, *Mater. Lett.*, 2007, **61**, 144.
17 Y. F. Yan, P. Liu, M. J. Romero and M. M. Al-Jassim, *J. Appl. Phys.*, 2003, **93**, 4807.
18 X. G. Wen, Y. P. Fang and S. H. Yang, *Angew. Chem., Int. Ed.*, 2005, **44**, 3562.
19 M. Armand, F. Endres, D. R. MacFarlane, H. Ohno and B. Scrosati, *Nat. Mater.*, 2009, **8**, 621.
20 F. Endres, *ChemPhysChem*, 2002, **3**, 144.
21 F. Endres, A. P. Abbott and D. R. MacFarlane, *Electrodeposition from Ionic Liquids*, Wiley-VCH, 2008.
22 Y. F. Lin and I. W. Sun, *J. Electrochem. Soc.*, 1999, **146**, 1054.
23 S.-P. Gou and I. W. Sun, *Electrochim. Acta*, 2008, **53**, 2538.
24 A. P. Abbott, J. C. Barron and K. S. Ryder, *Trans. Inst. Met. Finish.*, 2009, **87**, 201.
25 A. P. Abbott, G. Capper, K. J. McKenzie and K. S. Ryder, *J. Electroanal. Chem.*, 2007, **599**, 288.
26 T. J. Simons, A. A. J. Torriero, P. C. Howlett, D. R. MacFarlane and M. Forsyth, *Electrochem. Commun.*, 2012, **18**, 119.
27 N. M. Pereira, P. M. V. Fernandes, C. M. Pereira and A. F. Silva, *J. Electrochem. Soc.*, 2012, **159**, D501.
28 A. P. Abbott, J. C. Barron, G. Frisch, K. S. Rydera and A. F. Silva, *Electrochim. Acta*, 2011, **56**, 5272.
29 Z. Liu, S. Zein El Abedin and F. Endres, *Electrochim. Acta*, 2013, **89**, 635.
30 Z. Liu, A. Prowald, S. Zein El Abedin and F. Endres, *J. Solid State Electrochem.*, 2013, **17**, 1185.
31 C. Schonenberger, B. M. I. van der Zande, L. G. J. Fokkink, M. Henny, C. Schmid, M. Kruger, A. Bachtold, R. Huber, H. Birk and U. Staufer, *J. Phys. Chem. B*, 1997, **101**, 5497.
32 M. Motoyama, Y. Fukunaka, T. Sakka and Y. H. Ogata, *Electrochim. Acta*, 2007, **53**, 205.
33 Y. Konishi, M. Motoyama, H. Matsushima, Y. Fukunaka, R. Ishii and Y. Ito, *J. Electroanal. Chem.*, 2003, **559**, 149.
34 Y. Q. Liang, C. G. Zhen, D. C. Zou and D. S. Xu, *J. Am. Chem. Soc.*, 2004, **126**, 16338.